Local Production and Characterization of Biochar from Bamboo Waste and the Removal of Natural Organic Matter from Nakhon-nayok River, Thailand

Dusit Angthararuk[a,b]* Sasamol Phasuk[a] & Pannraphat Takolpuckdee[a]

[a] Science Education Department, Valaya Alongkorn Rajabhat University under the Royal Patronage, Pathum Thani, 13180 Thailand
[b] Faculty of Science and Technology, Suan Dusit University, Bangkok, 10300 Thailand

Abstract

The objective of this research was to produce a biochar from bamboo handicraft waste via pyrolysis process using modified 200 L steel drum kiln. A temperature outside the kiln-produced biochar appeared around 500-600 ^{o}C closely related to those of slow pyrolysis. The physical and chemical properties of bamboo biochar (BB) were characterized by using proximate and ultimate analysis, Brunauer−Emmett−Teller surface area techniques, elemental analysis, scanning electron microscopy coupled with an energy dispersive spectroscopy, Fourier transform infrared spectroscopy, Raman spectroscopy and X-ray diffraction. It was found that 28.76 ± 2.22 % of BB yield with 77.07 ± 1.92 % fixed carbon. As the morphology properties, its surface area and total pore were 247.5 ± 7.1 m^2.g^{-1} and 0.16 ± 0.02 cm^3.g^{-1}, respectively. Batch test for removal of natural organic matter (NOM) from real water, Nakhol-nayok River, by adsorbed on BB was studied. The results showed that the reducing percentages of dissolve organic matter (DOC) and absorbance at 254 nm wavelength (UV_{254}) at equilibrium were 71.33 ± 1.46 and 76.51 ± 2.01, respectively, while the adsorption capacity was 4.75 mg.g^{-1} DOC. Pseudo-second order kinetic model was the best suited for describing the adsorption of DOC onto BB. This suggests that interaction of NOM on BB were explored in terms of multicomponent adsorption, which the heterogeneous distribution of the adsorptive sites at biochar surfaces. This biochar is thus suitable for the adsorption of NOM from surface water and as a low cost effective adsorbent in the treatment of wastewater. The biochar can be applied for a variety of purposes for example: as biofuels, adsorbents, and as soil amendments. In addition the biochar kiln is also small and easy to create, no smoke, inexpensive, easy to use, don’t spend a lot of time and eco-friendly processing.

Keywords: Bamboo, Biochar, Characterization, NOM,

*** Corresponding Author**
e-mail: dusit_ang@dusit.ac.th

Introduction

High levels of natural organic matter (NOM) in surface water is a major concern for utilization of water, which causes color, smell, taste and microbial growth that the presence of NOM molecules can make water appear yellow or brown (Ghernaout et al., 2014). NOM is an intricate mixture of organic compounds from decomposed of microbial, plants and animals waste. NOM can be a source for the formation of carcinogens such as trihalomethanes (THMs) and haloacetic acids (HAAs) that water is disinfected with chlorine. The elimination of NOM is essential, which several physicochemical and biological methods, including, chemical precipitation, adsorption, filtration, reverse osmosis and coagulation, have been used for removal of NOM from water (Yehia & Said, 2021; Guillossou et al., 2020). However, these technologies encounter from several disadvantages stretching from the removal efficiency of low-concentration pollutants are incomplete resulting in toxic products, high energy, chemicals and maintenance consumption (He et al., 2017). Biochar adsorption is an interesting choice, eco-friendly and low-cost material that adsorbed many pollutants from contaminated water (Srivatsav et al., 2020). Biochar is a carbon-rich solid material produced from decomposed organic matter, agricultural residue, wood waste, municipal wastes and animal manures, by heating biomass precursors in an oxygen-limited environment (El-Hassanin et al., 2020; Wang et al., 2020; Yazdani et al., 2019). Biochar has been reported to be able to ameliorate soil fertility by carbon sequestration, increasing water and nutrient retention (Dokmaingam et al., 2020; Song et al., 2019; Kätterer et al., 2019), furthermore, to reduce greenhouse gas emissions into the atmosphere (Al-Ghussain, 2019; Zhang et al., 2017). Moreover, biochar can remove various contaminants, including pathogenic organisms, organic contaminants such as dyes (Nguyen et al., 2021) and inorganics such as heavy metals (Shaheen et al., 2019).

Bamboo is a local resource that is valuable to the way of life of Thai people from the past to the present. Because, bamboo is a fast-growing plant and multipurpose species which can be used from its rhizome/roots, clumps, shoots, leaves, leaf sheath, branch, and culm. The study on bamboo growing in Thailand found that the commercial bamboo cultivation areas are scattered throughout the country, amounting to 91,746 rai. (approx. 146.79 km^2) (Land Development Department, 2020). The Thai Wiang Community, Mueang District, Nakhon Nayok Province, Thailand (Fig. 1) has used bamboo in occupations such as handicraft, tree crutches and baked sticky rice in Bamboo. The bamboo residue, became community wastes were burnt out in open fields. The burning of these bamboo wastes contribute to global warming and increasing the level of airborne particles (Lohan et al., 2018). Greenhouse gases (GHG) emissions caused by the burning of agricultural crops in Mae Chaem Basin, Chiang Mai Province, Thailand, has been reported by Arunrat, Pumijumnong & Sereenonchai, (2018) that average values emission of CO_2, CO, CH_4, NO_x, SO_x $PM_{2.5}$ and PM_{10} were 9879.3, 253.0, 17.6, 11.7, 1.3, 29.3 and 39.1 kg ha^{-1} $year^{-1}$, respectively. It is a serious air pollution that negatively affects the environment and human health. The weakness of conventional charcoal production for example Earth kiln, pit kiln, brick kiln and horizontal 200 liter kiln are low quality of biochar due to the large amount of air entering the kiln during the burning process, long time operated for 1-3 days, smoke and inconvenient to use and move. The development of biochar kiln to produce quality biochar is interesting.

The objective of this research was to study the production of biochar from bamboo handicraft waste by local drum kiln via pyrolysis process and investigated their properties and its application for removal of natural organic matter from Nakhol-nayok River, Thailand.

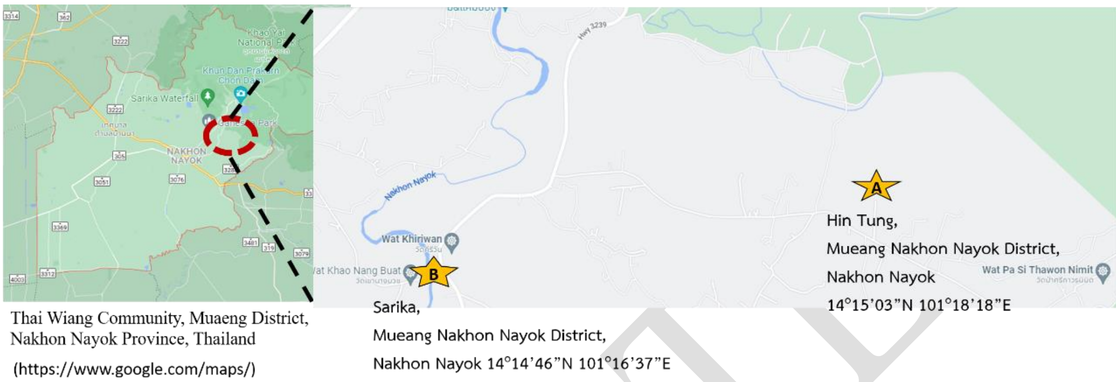

Fig. 1 Map of the Thai Wiang Community, Mueang District, Nakhon Nayok Province, Thailand; the place of (A) biochar production, (B) collected surface water from Nakhon Nayok river, by Google Earth™ mapping

Materials and methods

1. Bamboo biomass

The bamboo handicraft waste used to feedstock for biochar production, were collected from local area at Hin Tung, Mueang Nakhon Nayok District, Nakhon Nayok Province (14º15'03"N 101º18'18"E) showed in Fig.1 A. The dirt, sand and unwanted material from the surface of bamboo waste sample were removed, after that dried in an open air for a week.

2. Biochar production

Bamboo biochar (BB) was produced using a portable low cost container steel drum kiln with available local resources for easy operation of local farmers following the design of O'Toole (2013). The kiln was modified by added air vents at bottom and upper zone furthermore used 100 L of steel drum as flue for increasing air flow. About 18 kg of bamboo materials (<10% moisture content) were filled in a small container (A) as measuring 0.66 m in height and 0.37 m diameter then close the lid tightly to prevent oxygen entering during the pyrolysis process. The small container was then placed down inside a larger container (B) (0.88 m height and 0.59 m diameter) (Fig. 2). Approximately 20 kg of other bamboo wastes were loaded to gap between the containers A and B which was burned to heating the inner container. The steel drum (C) was taken to cover the top to increase the air flow in the combustion after igniting bamboo (3-5 min). The combustion temperatures surrounding, 3 positions in each of 3 zones of the outer chamber were measured by non-contact handheld infrared thermometer (MESTEK IR01D). The biochar yield was calculated as follows: production yield (wt %) = (W_{BB}/W_{bamboo}) x 100, where W_{BB} was the weight of BB (kg) and W_{bamboo} was the weight of the bamboo biomass feedstock (kg) loaded into the kiln, both on a basis of dry weight. After all the outer container wood waste had burnt up (≈60 min) and left to cool. The BB product was taken to study the physical and chemical properties.

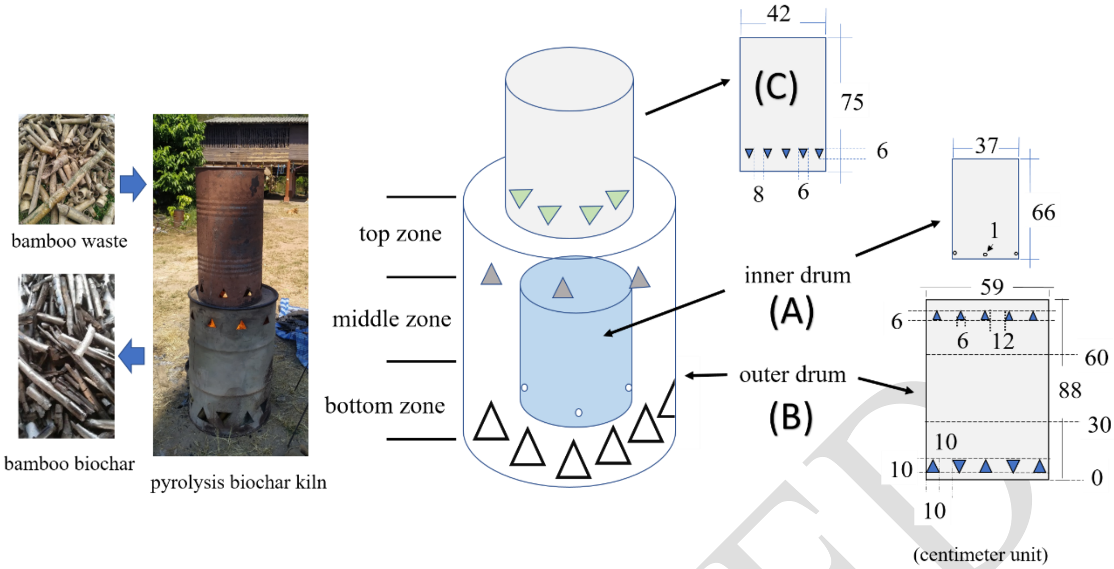

Fig. 2 Schematic diagram of bamboo biochar production

3. Characterization of BB

Proximate analysis

Proximate analysis is the composition of the moisture, ash, volatile matter and fix carbon were analyzed by modified according to Aller, Bakshi, & Laird (2017). The moisture content of BB was determined based on weight loss after two hours at 110 °C in hot air oven (Memmert, Germany) under N_2 purge. Volatile matter (VM) of BB (same sample) was carried out by heating a crucible containing the BB covered with ceramic lid placed in a stainless steel box under nitrogen purge by muffle furnace to 950°C held 10 min at heating rate 2 °C min^{-1} (THERMCONCEPT Ht40 Al, Germany). Ash content of BB was measured based on weight loss by heating the same samples to 730 °C in an air atmosphere using the same muffle furnace and perform overnight (8-10 hours). After the ashing, the furnace was then switched off and let cool before the sample was transferred to a desiccator. The moisture (% Moisture), volatile matter (% VM) and ash (% Ash) content were determined as follows by equations 1, 2 and 3, respectively.

$$\%\,Moisture = \left(\frac{W_I - W_D}{W_D}\right) * 100 \qquad \text{(Eq. 1)}$$

$$\%\,VM = \left(\frac{W_D - W_V}{W_D}\right) * 100 \qquad \text{(Eq. 2)}$$

$$\%\,Ash = \left(\frac{W_A}{W_D}\right) * 100 \qquad \text{(Eq. 3)}$$

Where W_I, W_D, W_V and W_A were the weight (g) of BB of initial, oven drying at 110 °C, after heat at 950 °C and after combustion at 730 °C overnight, respectively. Whereas, the fixed carbon is the carbon found in the biochar, which is left after moisture, volatiles and ash in the biochar are driven off. The percent fixed carbon (% FC) was calculated as follows by equation 4.

$$\%\,FC = 100\% - (\%\,Moisture + \%\,VM + \%\,Ash) \qquad \text{(Eq. 4)}$$

Ultimate analysis

The specific surface area and total pore volume of BB were analyzed by N_2 adsorption-desorption by Autosorb 1MP surface area analyzer, Quantachrome Instruments, USA. The BB sample was degassed under vacuum at 250 °C performed overnight in order to eliminate the volatile matters before measuring. An elemental analyzer was used to determine CHN/O compositions (a LECO CHNS model 932 elemental analyzer) through pyrolysis. The both techniques were analyzed by The Petroleum and Petrochemical College, Chulalongkorn University, Thailand. The oxygen content was calculated by difference. The pH value of BB was measured by a Starter 3100 bench, Ohaus pH meter. A 2 grams of BB was added in 50 cm^3 double distilled water, the mixture was shaken for 30 minutes at 150 rpm, then centrifuged and filtered. The filtrate was tested for the pH value.

Scanning electron microscopy (SEM) and Energy-dispersive X-ray spectroscopy (EDS)

Scanning electron microscopy (SEM) and energy-dispersive X-ray spectroscopy (EDS) techniques allow for targeted analysis of sample surfaces that offer us a direct way to observe the surface structure and mineral distribution of biochar. The BB surface morphology was investigated using a JEOL SEM analyzer JSM-6610 LV (JEOL Ltd., Tokyo, Japan) with an accelerating voltage of 20 kV. Meanwhile, the surface chemical elemental composition was determined by Energy Dispersion Spectrometry analysis (EDS, Oxford instrument X-Max 50 mm^2, England).

Infrared spectroscopy

Attuned total reflectance (ATR) Fourier transform infrared spectroscopy (FTIR) was carried out to determine the functional groups of both the BB and feedstock. ATR-FTIR was performed using an IR Tracer-100 FTIR spectrophotometer (Shimadzu) with a diamond, zinc selenide (ZnSe) prism was used in the ATR accessory. The number of scans was 40, with wide range at 4000 to 500 cm^{-1} at a resolution of 4 cm^{-1}. The background was collected before each measurement. The band positions were obtained using the LabSolutions IR control software.

Raman spectroscopy

Raman spectra of BB was carried out by using a Horiba LabRAM HR Evolution Raman Spectrometer. The spectra were acquired with a 50 LWD objective that were recorded from 650-2200 cm^{-1} with an excitation laser source of 532 nm, 100 mW, 3.2 to 5% power and using 20 accumulations. The instrument was controlled using LabSpec 6 software.

X-ray diffraction (XRD)

X-ray diffraction (XRD) analysis was used to investigate any crystallographic structure in the biochar. XRD pattern of the BB sample was identified using a Bruker D2 Phaser X-ray diffractometer (Bruker, Karlsruhe, Germany). It was operated in the 2θ of range 10-90° at 1° min^{-1} scan speed and step time 0.5° at room temperature.

Batch adsorption experiment

Surface water was collected from Nakhol-nayok River, Sarika, Mueang Nakhon Nayok District, Nakhon Nayok Province, Thailand (14°14'46"N 101°16'37"E) shown Fig. 1 in August, 2021. The physicochemical characteristics of raw water were as follows: pH: 7.54, DO 1.70-8.00, BOD 1.03-3.23 and N_{NH_3} 0.01-1.43 mg L^{-1} (Regional Environmental Office 7, 2021). A 100 liters surface water were collected with a black polyethylene container then brought to the laboratory. Pre-treatment, the water sample were filtered through 5 and 1 µm commercial polypropylene filter, 0.7 µm GF/C, 0.45 µm cellulose nitrate membrane (Whatman) and RO Membrane (ULTRATEK TW-1812-50 GPD) that showed in Fig. 3. Batch experiments were performed with NOM adsorption in an aqueous solution, 100 cm^3 of sample water and 1 $g{\cdot}L^{-1}$ black powder adsorbent were placed in Erlenmeyer flasks (250 mL) shaking with 150 rpm at room temperature without pH adjustment. The kinetic was studied at intervals that varied between 1 minute and 48 hours. The collected samples after batch test were centrifuged at 3,000 rpm for 5 min before being filtered through 0.45 µm nylon syringe membranes to NOM measurement. In order to assess the NOM removal efficiency of BB was analyzed for dissolved organic carbon (DOC) using Multi N/C 2100S-Direct injection TOC analyzer (Analytik Jena GmbH, Germany) and for absorbance at 254 nm wavelength (UV_{254}) in 1 cm quartz cells (Kearns et al., 2021), by a UV-1201 Shimadzu spectrophotometer. The efficiency removal of NOM and adsorption capacity were calculated as follows by equations 5 and 6, respectively.

$$\%\, NOM\ removal = \left(\frac{C_i - C_t}{C_i}\right) * 100 \qquad \text{(Eq. 5)}$$

$$Adsorption\ capacity, Q_t(mg.g^{-1}) = \frac{(C_i - C_t)}{W} V \qquad \text{(Eq. 6)}$$

Where C_i and C_t (mg.L^{-1}) were DOC concentration at initial and at time t, respectively, V (L) was mixture volume, and W (g) was BB weight. The other hand, the NOM removal in UV_{254} absorption was calculated as: removal (%) = [(A_0-A_t)/A_0] * 100, where A_0 and A_t were the absorbance at 254 nm at time 0 and t, respectively.

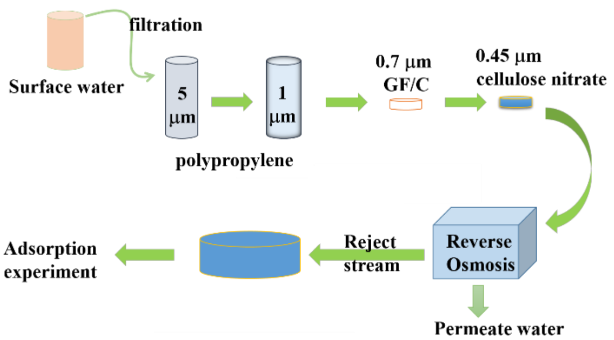

Fig. 3 Diagram prepare surface water sample to batch adsorption experiment.

Results and discussion

Temperature Profile and Production Yield

Performance of the pyrolysis system has been defined in terms of reactor temperature profile, biochar yield, and characteristics of biochar obtained. The averages temperature for different position on the outside of kiln were shown in Fig. 4. The results showed that the average of 3 zones outside temperature of the kiln obviously increased with time. The maximum temperatures, top zone, middle zone and bottom zone of the kiln were 610.8, 605.4 and 597.3 °C, respectively as a result of heat transfer from combustion of fuel bed at the top to bottom. It can be observed that the temperature of all zone increased from room temperature to maximum with increasing time over 35 min and then decreased to 40 ± 1 °C over 80 min. However, the inner container should not be opened, it's left for 2 hours, because biochar can ignite again. The process was observed to complete in about 4 hours. The percent average BB yield was 28.76 ± 2.21 from six pyrolysis batches. Proximate and ultimate analysis was carried out to evaluate the characteristics of the BB showed in Table 1.

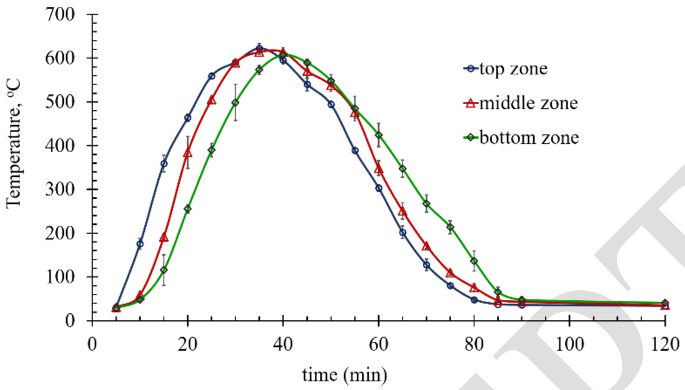

Fig.4 The temperature profile of the outside kiln for different position

During pyrolysis process, cellulose, hemicellulose, lignin and fat of the biomass were thermally disintegrated over the temperature range between 150 and 400 °C to increase the carbon content by destroying oxygen, hydrogen and non-carbon species to gaseous products formed (Conte et al., 2021). After that, an acid compounds, ketones, aldehydes, phenols, furans, and guanidines would be formed over the temperatures between 400 and 700 °C (Lewandowski et al., 2020). The weight loss of biomass from the thermal conversion to biochar was associated with decomposition of carbonates, sulfates and hydroxides, hydroxylation of some oxide compounds that affected to the surface area and pore of BB. A surface analysis which specific surface area and pore volume of BB in this studied were 247.5 ± 7.1 $m^2.g^{-1}$ and 0.16 ± 0.02 $cm^3.g^{-1}$, respectively. The drum kiln was developed from the traditional kiln and was widespread to use for the biochar production in developing countries. Batch simple kiln technologies are likely of the first choice for small farmers and start-up biochar producers before it can be improved into a large system that is widespread and has affordable price. In India and East Africa, forests are sustainably managed for biochar production using low-cost kiln as well as being more environmentally friendly that can reduce GHG emissions into the atmosphere by approximately 75%. Moreover, increased efficiency of biochar production was about 30%-40% better than the traditional biochar production method, which was about 10%-20% (Adam, 2009). Similarly, the kiln in this studied, all wood gases released during carbonization were controlled and burned as a fuel for the process to reduce emissions.

Table 1 Physical and chemical properties of the BB

Bamboo biochar properties	% dry weight
Proximate analysis[a]	
Biochar yield	28.76 ± 2.22
Ash	6.58 ± 2.00
Moisture content	7.32 ± 1.00
Volatile	9.03 ± 1.77
Fix carbon	77.07 ± 1.92
pH	8.90 ± 0.51
Specific surface area (m^2/g)[b]	247.5 ± 7.1
Pore volume (cm^3/g)[b]	0.16 ± 0.02
Elemental analysis [b]	
C	65.17 ± 2.15
H	3.16 ± 0.05

N	0.77 ± 0.06
O*	30.94 ± 2.15
H/C	0.04
O/C	0.47

[a] n = 6, [b] n = 3, * By difference

Physical and chemical properties of the BB

Table 1 has been showed the elemental analysis, CHN/O chemical properties of the BB. The ratio of hydrogen to carbon (H/C) indicates aromaticity index to evaluate the degree of thermochemical change that produces fused aromatic ring structures in biochar while oxygen to carbon ratio (O/C) represents hydrophilicity index relate to biochar stability. In the pyrolysis process, carbon, hydrogen and oxygen are eliminated in gases and volatiles matter, as a result, the H/C and O/C ratios would be decrease that corresponding to increase in aromaticity and carbon content with the increasing in pyrolysis temperature (Windeatt et al., 2014). The lower of H/C and O/C ratio used to indicate higher fused aromatic ring structure and higher stability in carbon fraction (Fernandes et al., 2020). The H/C and O/C ratio of BB in this study were 0.04 and 0.47, respectively, indicated a high carbon content and higher stability in aromatic ring structures would be preserved at least 100 years in soil. This was consistent with the work done by Spokas (2010), which showed the O/C ratio in the range of 0.2–0.6. That would mean the dwell time of biochar in soil about 100–1000 years.

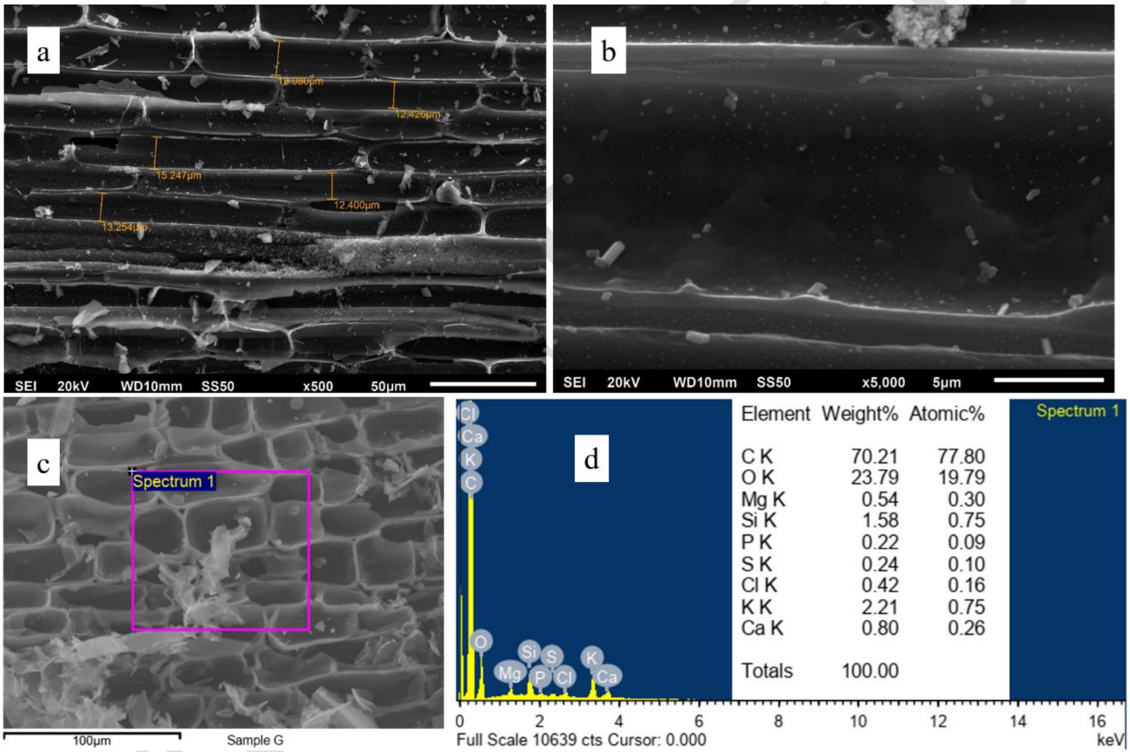

Fig. 5 SEM images of bamboo biochar: a and b were 500 and 5000 times magnification, respectively, c and d were EDS analysis

The BB morphological characteristics obtained by scanning electron microscopy (SEM) and energy dispersive x-ray spectroscopy (EDS) showed in Fig. 5. That can be seen obvious morphological of BB with a large surface area, tubular shapes, rough surface structures and sharp edges, an approximate porous space of 12-15 μm spread on biochar surface (Fig. 5a). Moreover, at a magnification of 5,000X, a micropore was found within the mesopores in Fig. 5b. The BB cross-section appeared mesopores structure spread on biochar surface and the surface pore morphology as a honeycomb-like structure (Fig. 5c). The results of the SEM images of BB were corresponding with the results of the surface analysis which specific surface area and pore volume, as influenced to the content of water and nutrients retained (Hernández-Mena, L., Pécora, A., & Beraldo, A., 2014). The C (76.32 %) and O (16.77 %) content as the major elements of the BB were indicated by EDS analysis showed in EDS analysis (Fig 5d). Furthermore, the other mineral, such as Mg, Si, P, S, Cl, K, and Ca could be detected form six pyrolysis batches appeared in Table. 2. These results pointed to the C was the main skeleton with O in the BB, which may drive from oxygen-containing compounds (e.g. carboxylic -COOH, hydroxyl -OH, carbonate $-CO_3^{2-}$, phosphate $-PO_4^{3-}$or sulphate $-SO_4^{2-}$).

Table. 2 Element composition of BB by EDS analysis

Element	Average
C	76.32 ± 3.25
O	16.77 ± 3.02
Mg	0.43 ± 0.17
P	0.56 ± 0.16
Cl	0.61 ± 0.71
K	3.43 ± 3.28
Ca	0.64 ± 0.01
S	0.35 ± 0.14
Si	1.57 ± 1.60

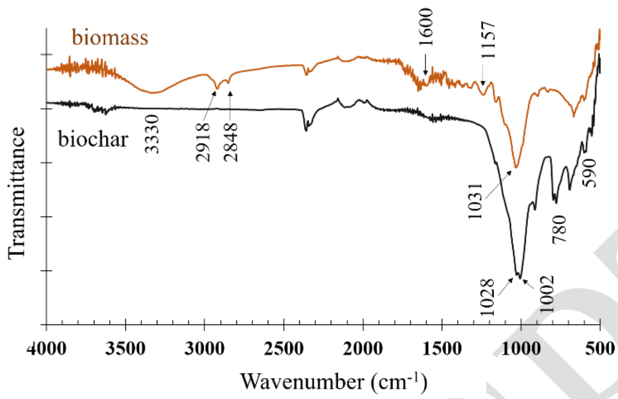

Fig. 6 ATR-FTIR spectra of raw bamboo biomass and its biochar

ATR-FTIR spectra of biomass and BB was shown in Fig. 6. Lignocellulosic materials consist of cellulose, hemicellulose and lignin indicated broad band between 3500 and 3000 cm^{-1} corresponded with O-H and N-H vibrations of phenol and amine and the C-H symmetric stretching at 2918 and 2848 cm^{-1} (Qin et al., 2020). The bamboo-derived biochars, the band at the region at 3000-3500 cm^{-1} disappeared that signifies complete dehydration and de-oxygenation reactions at 600 °C pyrolysis temperature. Recommending a polar functional groups were reduced to hydrophobic material with very less functional groups were obtained (Ramola et al., 2014). The fingerprint region (1600 to 400 cm^{-1}) provides more insights for disappearance of cellulose and hemicellulose in BB sample owing to the decomposition of the raw biomass. The spectra of biomass, a peak at 1600 cm^{-1} was assigned to the aromatic skeletal C=C and C=O vibration mode of hemicellulose and lignin (Nair, Mondal & Weichgrebe, 2020). The peak at 1031 cm^{-1} referred to the C-OH or C-O-C stretching vibrations of cellulose, hemicellulose, and lignin (El-Sakhamed et al., 2018). Peaks for C–H bending bonds (out of plane) in the region of 900–675 cm^{-1}, which was characteristic of the aromatic substitution pattern, were clearly visible for biochars. The peak at 1000 cm^{-1} can be assigned to the C-O stretching vibration of alcohols and ester groups (Guizani et al., 2017). Silicates (Si-O) and phosphates (P-O) were displayed at the wideband around 1000 cm^{-1} that remain unchanged at temperatures below 700 °C (Zhang et al., 2015 and Cantrell et al., 2012). The 590 cm^{-1} peak obtained from iron oxide compounds or Fe–O–Si bond (Gotić & Musić, (2007) that forms in attendance of iron and silicate minerals at higher temperatures.

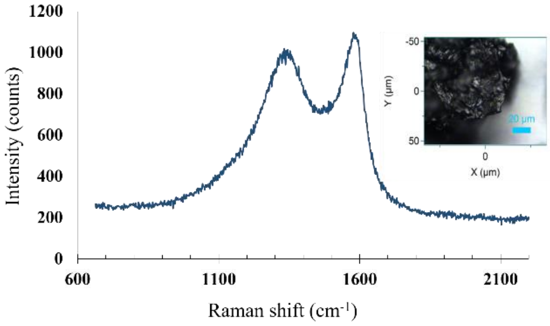

Fig. 7 Raman spectrum of bamboo biochar

Raman Spectroscopy is an outstanding method for characterizing carbon materials. Raman spectrum of the BB appeared a maximum intensity at 1348 cm^{-1} and 1588 cm^{-1} that in accordance with the D and G bands of the graphitic-like structures, respectively, shown in Fig. 7. Both D and G peaks are the result of vibrations of sp^2-bonded carbon atoms (Gonzalez-Canche et al., 2021). The D band is due to out of plane vibrations of sp^2-bonded carbon attributed to the presence of structural defects whereas the G band is formed by sp^2 bonded crystallite carbon vibration both in rings and chains of the graphite crystalline plane. (Ferrari & Robertson, 2000). The intensity ratio between the D and G bands can be used to estimate the degree of crystallinity of carbon-containing materials. The high D/G intensity ratio of BB was 0.868 (in Fig. 7) that indicating the pyrolysis temperature greater than 600 ^oC (Gonzalez-Canche et al., 2021).

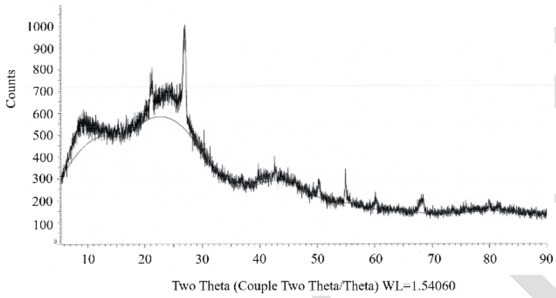

Fig. 8 XRD characterization of bamboo biochar

X-ray diffraction analysis is performed to assess a degree of crystalline or amorphous structure in a sample. The XRD diffractogram of BB contained mainly the amorphous compounds was indicated in Fig. 8. The two theta (2θ) wide rang 20˚–30˚refers to the stacking structure of the aromatic layer (Liu et al., 2012). Sharp crystalline non-labeled peaks in BB diffractogram probably indicated of miscellaneous inorganic components, such as these peaks is consistent with the higher content of SiO_2 (quartz, 2θ = 20.86˚, 26.62˚) and $CaCO_3$ (calcite, 2θ = 50.58˚), correspondingly with Sackey et al., (2021) work done.

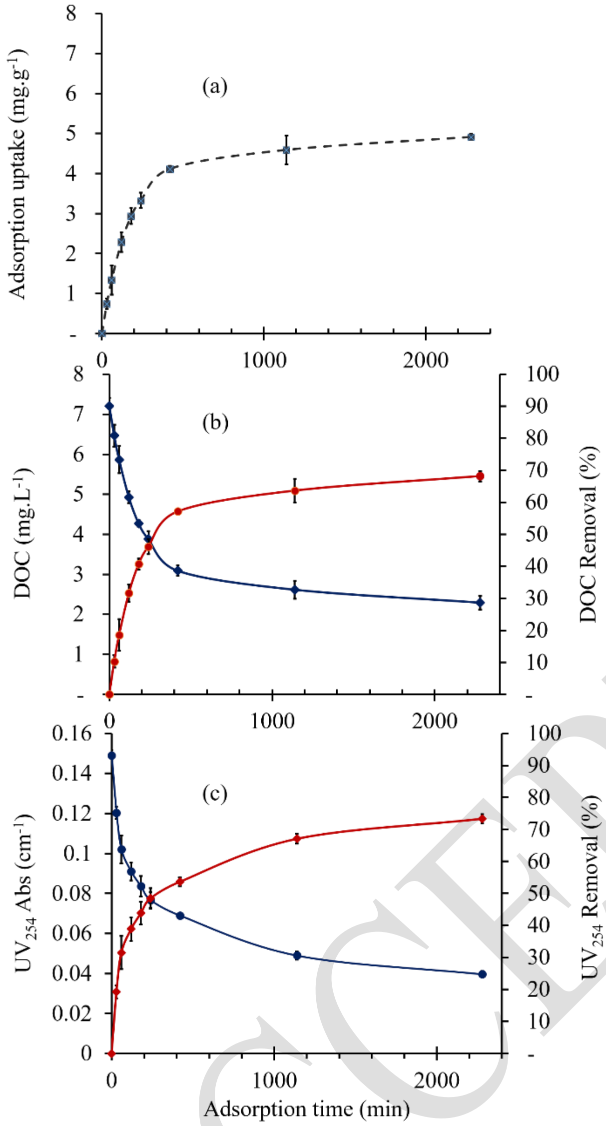

Fig. 9 NOM removal, (a) adsorption efficiency, (b) DOC reducing, (c) UV_{254} absorbance reducing

Removal of NOM

Application of BB for NOM removal from Nakhol-nayok River, Thailand was investigated. The amount of NOM was represented in DOC concentration and UV absorbance at 254 nm measurement. The initial content of DOC and UV_{254} were 7.21 ± 0.20 $mg.L^{-1}$ and 0.149 ± 0.002 cm^{-1}, respectively that high values of DOC and UV_{254} due to the samples collected in August, which the rainy seasons, related to since soils rich in organic matter was transported into the water by run-off (Singh and Choden, 2014). The effect of adsorption time on the removal of NOM was shown in Fig. 9. The adsorption capacity of the DOC on BB increased with the extension of contact time. In the first 6 hours the adsorption capacity grew rapidly after that the adsorption tended to equilibrium gradually (Fig 9(a)) and the adsorption efficiency of at equilibrium was 4.75 $mg.g^{-1}$. Figure 9 (b) and (c) showed that the adsorption rate of DOC and UV_{254} on BB were initially fast and then gradually reduced until equilibrium reached. More than 50% of DOC and UV_{254} were removed with 6 hours contact time of 1 $g.L^{-1}$ BB in first stages. A slower phase occurred thereafter onward to the equilibrium was achieved within 48 hours, corresponding to about 70% removal all both.

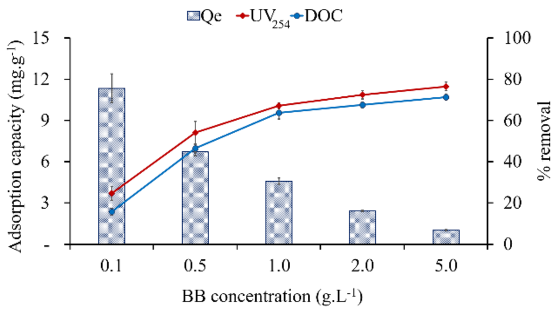

Fig. 10 Effect of adsorbent concentration on DOC adsorption

Effect of BB dose was evaluated by varying adsorbent dosage in the range from 0.01 to 0.5 g of adsorbent in 100 cm^3 water sample. It is clear from Fig. 10 that the removal percentage of the DOC and UV_{254} direct proportional to adsorbent dosage from 15.71 ± 1.44 to 71.33 ± 1.46% and 24.60 ± 3.31 to 76.51 ± 2.01, respectively. Whereas the adsorption efficiency of DOC on BB at equilibrium (Q_e) decreased from 11.33 ± 1.04 to 1.03 ± 0.02 $mg.g^{-1}$ with the increasing in adsorbent dose 0.1 to 5.0 $g.L^{-1}$ shown in Fig.10. The enlarged of the adsorbent dose effected the number of active sites increases and thus removal percentage improved. However, the adsorbent high content may be to aggregation of adsorbent would lead to a reduction in the adsorbent capacity through decreasing the total surface area that causing the site to be less active which results in the less number of DOC molecules per active site.

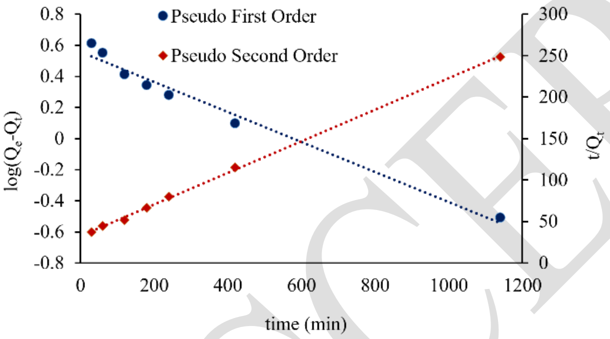

Fig. 11 Adsorption kinetic model of DOC removal

The adsorption kinetics of BB was educated based on the above adsorption equilibrium results of DOC. The adsorption kinetic model of DOM onto BB was assessed by using pseudo-first-order and pseudo-second-order kinetic models as follows by equations 7 and 8, respectively.

$$log\ (Q_e - Q_t) = logQ_e - \frac{k_1}{2.303}t \qquad \text{(Eq. 7)}$$

$$\frac{t}{Q_t} = \frac{1}{k_2 Q_e^2} + \frac{1}{Q_e}t \qquad \text{(Eq. 8)}$$

Where Q_e and Q_t are the biochar adsorption uptake ($mg.g^{-1}$) at equilibrium time and any time t (min), respectively, the adsorption rate constants k_1 (min^{-1}) and k_2 ($g.mg^{-1}.min^{-1}$) are primary and secondary constants, respectively. A plotting of log (Q_e-Q_t) versus time in Eq.7 and of t/Q_t versus time in Eq.8 both yields a straight line showed in Fig. 11. The rate constant (k_1) and absorption capacity (Q_e) of the pseudo-first-order reaction can be determined from the slope of the straight line and intercept of the plot in Fig. 11 (blue line), respectively. Similarly, the rate constant (k_2) and equilibrium absorption capacity (Q_e) of the pseudo-second-order reaction were determined from the intercept and slope of a linear relationship in Fig. 11 (red line). According to the equation 7 and 8 given above, the kinetic parameters were calculated to appearing in Table 3. It was clear from the correlation coefficient, R^2 values given in the Table 3 that pseudo-second-order kinetic model was greater than pseudo-first-order kinetic model, which the best describe the adsorption of DOC on BB. This suggests that interaction of NOM on BB were explored in terms of multicomponent adsorption of its different fractions as chemical nature, functional groups present on the surface, pore filling, π–π interactions, polar/electrostatic interactions, hydrophobic effect, and hydrogen bonding. (Yazdani et al., 2019; Ahmad et al., 2014)

Table. 3 Adsorption kinetic parameters of DOC on BB

parameter	pseudo-first-order	pseudo-second-order
Adsorption rate constant, k	0.0023 (min^{-1})	0.0011 ($g.mg^{-1}.min^{-1}$)
Q_e ($mg.g^{-1}$)	3.607	5.254
R^2	0.9783	0.9992

Conclusion

The production temperature (500–600°C) and heating time about 1 hour for biochar produced in our kiln were most closely related to the slow pyrolysis. The process was observed to complete in about 4 hours with the % BB yield was 28.76 ± 2.21 of dry weight. The BB high quality were characterized by BET, SEM-EDS, ATR-FTIR, Raman spectroscopy, XRD, proximate analysis and elemental composition revealed macro- meso- and micro-pore structure, high surface area was 247.5 ± 7.1 $m^2.g^{-1}$ and 0.16 ± 0.02 $cm^3.g^{-1}$ of pore volume, 77.07 ± 1.92 % fix carbon , amorphous structure mixed of sp^2 and sp^3 carbon bonds and surface functionality. The absorbent product was applied to remove NOM from Nakhol-nayok River, Thailand, it can be reduce 50% at 6 hours contact time with 1 $g.L^{-1}$ of BB. The absorption efficiency at equilibrium and maxima removal ware 4.75 $mg.g^{-1}$ and about 70 %, respectively followed pseudo-second-order kinetic model. Next opportunity, BB may be used to eliminate heavy metals in local community groundwater. Notwithstanding this results cannot be generalized across kiln design and starting biomass feedstock nevertheless it represents that our simple kiln can produce good quality biochar from bamboo wastes. In addition the biochar kiln is also small and easy to create and use, no smoke, inexpensive, don't spend a lot of time and eco-friendly processing.

Acknowledgment

This research was supported by Suan Dusit University, Thailand

References

Adam, J.C. (2009) Improved and more environmentally friendly charcoal production system using a low-cost retort–kiln (Eco-charcoal), *Renew Energ, 34,* 923–925

Ahmad, M., Rajapaksha, A.U., Lim, J.E., Zhang, M., Bolan, N., Mohan, D., Vithanage, M., Lee, S.S., & Ok, Y.S. (2014) Biochar as a sorbent for contaminant management in soil and water: a review, *Chemosphere, 99,* 19–33.

Al-Ghussain L. (2019) Global warming: review on driving forces and mitigation. (2019) *Environ. Prog. Sustain., 38,* 13–21

Aller, D., Bakshi, S., & Laird, D.A. (2017). Modified method for proximate analysis of biochars. *J. Anal. Appl. Pyrolysis., 124,* 335-342.

Arunrat, N., Pumijumnong, N., & Sereenonchai, S. (2018) Air-Pollutant Emissions from Agricultural Burning in Mae Chaem Basin, Chiang Mai Province, Thailand. *Atmosphere, 9,* 145. https://doi:10.3390/atmos9040145.

Cantrell, K.B., Hunt, P.G., Uchimiya, M., Novak, J.M., & Ro, K.S. (2012) Impact of pyrolysis temperature and manure source on physicochemical characteristics of biochar. *Bioresour Technol, 107,* 419–428. https://doi.org/10.1016/j.biortech.2011.11.084

Conte, P., Bertani, R., Sgarbossa, P., Bambina, P., Schmidt, H.-P., Raga, R., Lo Papa, G., Martino, D.F.C., & Lo Meo, P. (2021) Recent Developments in Understanding Biochar's Physical–Chemistry. *Agronomy, 11,* 615. https://doi.org/10.3390/agronomy11040615

Dokmaingam, P., Kongkratoke, S., Anuwatnonthakate, A., & Yongprapat, S. (2020) The Improvement of Hydroponics Growth Media by Using the Corncob Biochar, *Journal of Food Health and Bioenvironmental Science, 13(3),* 26-31

El-Hassanin, A.S., Samak, M.R., Radwan, S.R., & El-Chaghaby, G.A. (2020) Preparation and characterization of biochar from rice straw and its application in soil remediation. *Environ. Nat. Resour. J., 18(3),* 283-289. https://doi: 10.32526/ennrj.18.3.2020.27

El-Sakhawy, M., Kamel, S., Salama, A., & Tohamy, H.-A.S (2018) Preparation and infrared study of cellulose based amphiphilic materials. *Cellulose Chem. Technol., 52(3-4),* 193-200.

Fernandes, B.C.C., Mendes, K.F., Dias Júnior, A.F., da Silva Caldeira, V.P., da Silva Teófilo, T.M., Severo Silva, T., Mendonça, V., de Freitas Souza, M., & Valadão Silva, D. (2020) Impact of Pyrolysis Temperature on the Properties of Eucalyptus Wood-Derived Biochar. *Materials. 13(24),* 5841. https://doi.org/10.3390/ma13245841.

Ferrari, A.C., & Robertson, J. (2000) Interpretation of Raman Spectra of Disordered and Amorphous Carbon. *Phys. Rev. B, 61,* 14095–14107.

Gao, M., Zhu, L., Peh, C.K., & Ho, G.W. (2019) Solar Absorber Material and System Designs for Photothermal Water Vaporization towards Clean Water and Energy Production. *Energy Environ. Sci., 12,* 841–864. https://doi:

10.1039/c8ee01146j
Ghernaout, D., Moulay, S., Ait Messaoudene, N., Aichouni, M., Naceur, M.W., & Boucherit, A. (2014) Coagulation and Chlorination of NOM and Algae in Water Treatment: A Review. *Int J Environ Monit Anal, 2,* 23-34. https://doi.org/10.11648/j.ijema.s.2014020601.
Gonzalez-Canche, N.G., Carrillo, J.G., Escobar-Morales, B., Salgado-Tránsito, I., Pacheco, N., Pech-Cohuo, S.C., & Peña-Cruz, M.I. (2021) Physicochemical and Optical Characterization of Citrus aurantium Derived Biochar for Solar Absorber Applications. *Materials, 14,* 4756. https://doi.org/10.3390/ma14164756
Gotić M, & Musić S (2007) Mössbauer, FT-IR and FE SEM investigation of iron oxides precipitated from $FeSO_4$ solutions. *J Mol. Struct., 834-836*, 445–453. https://doi.org/10.1016/j.molstruc.2006.10.059
Guillossou, R., Le Roux, J., Mailler, R., Pereira-Derome, C.S., Varrault, G., Bressy, A., Vulliet, E., Morlay, C., Nauleau, F., Rocher, V., & Gasperi, J. (2020) Influence of dissolved organic matter on the removal of 12 organic micropollutants from wastewater effluent by powdered activated carbon adsorption. *Water Res., 172,* 115487. https://doi: 10.1016/j.watres.2020.115487.
Guizani, C., Jeguirim, M., Valin, S., Limousy, L., & Salvador, S. (2017) Biomass Chars: The Effects of Pyrolysis Conditions on Their Morphology, Structure, Chemical Properties and Reactivity. *Energies. 10(6),* 796. https://doi.org/10.3390/en10060796
He, J., Li, Y., Cai, X., Chen, K., Zheng, H., Wang, C., Zhang, K., Lin, D., Kong, L., & Liu, J. (2017) Study on the removal of organic micropollutants from aqueous and ethanol solutions by HAP membranes with tunable hydrophilicity and hydrophobicity. *Chemosphere, 174,* 380–389.
Hernández-Mena, L., Pécora, A., & Beraldo, A. (2014) Slow pyrolysis of bamboo biomass: analysis of biochar properties. *Chem. Eng. Trans., 37,* 115-120. http://doi:10.3303/CET1437020
Kätterer, T., Roobroeck, D., Andrén, O., Kimutai, G., Karltun, E., Kirchmann, H., Nyberg, G., Vanlauwe, B., & Nowina, K.R. (2019) Biochar addition persistently increased soil fertility and yields in maizesoybean rotations over 10 years in sub-humid regions of Kenya. *Field Crops Res., 235,* 18–26. https://doi.org/10.1016/j.fcr.2019.02.015
Kearns, J., Dickenson, E., Aung, M.T., Joseph, S.M., Summers, S.R., & Knappe, D. (2021). Biochar water treatment for control of organic micropollutants with UVA surrogate monitoring. *Environ. Eng. Sci. 38,* 298-309. https://doi.org/10.1089/ees.2020.0173
Land Development Department, (2020). *The proportion of area under bamboo cultivation in various regions of the country*. Retrieved from: http://www1.ldd.go.th/WEB_OLP/Lu_62/Lu62_C/NYK2562.htm
Lewandowski, W.M., Ryms, M., & Kosakowski, W. (2020) Thermal Biomass Conversion: A Review. *Processes, 8(5),* 516. https://doi.org/10.3390/pr8050516
Liu, Y., Zhao, X., Li, J., Ma, D., & Han, R. (2012) Characterization of bio-char from pyrolysis of wheat straw and its evaluation on methylene blue adsorption, *Desalination Water Treat., 46(1-3),* 115-123 http://dx.doi.org/10.1080/19443994.2012.677408
Lohan, S.K., Jat, H.S., Yadav, A.K., Sidhu, H.S., Jat, M.L., Choudhary, M., Peter, J.K., & Sharma, P.C., (2018) Burning issues of paddy residue management in north-west states of India. *Renew. Sustain. Energy Rev. 81,* 693-706. https://doi.org/10.1016/j.rser.2017.08.057.
Nair, R.R., Mondal, M.M. & Weichgrebe, D. (2020) Biochar from co-pyrolysis of urban organic wastes-investigation of carbon sink potential using ATR-FTIR and TGA. *Biomass Conv. Bioref.* https://doi.org/10.15488/10722.
Nguyen, T.T., Chen, H.-H., To, T.H., Chang, Y.-C., Tsai, C.-K., Chen, K.-F., & Tsai, Y.-P. (2021) Development of Biochars Derived from Water Bamboo (Zizania latifolia) Shoot Husks Using Pyrolysis and ultrasound-Assisted Pyrolysis for the Treatment of Reactive Black 5 (RB5) in Wastewater. *Water, 13,* 1615. http://doi.org/10.3390/w13121615
O'Toole, A., Zarruk, K., Steffens, M., & Rasse, D.P. (2013) Characterization, stability, and plant effects of kiln-produced wheat straw biochar. *J Environ Qual., 42(2),* 429-36. https://doi: 10.2134/jeq2012.0163.
Qin, L., Wu, Y., Hou, Z., & Jiang, E. (2020) Influence of biomass components, temperature and pressure on the pyrolysis behavior and biochar properties of pine nut shells. *Bioresour. Technol. 313,* 123682. https://doi.org/10.1016/j.biortech.2020.123682.
Ragional Environmental Office 7 (2021) *Report: surface water quality*, Retrieved from: http://www.reo07.mnre.go.th/th/information/list/2051
Ramola, S., Mishra, T., Rana, G. S. & Srivastava, R. K. (2014) Characterization and pollutant removal efficiency of biochar derived from baggase, bamboo and tyre. *Environ Monit Assess 186,* 9023–9039. https://doi.org/10.1007/s10661-014-4062-5
Ronsse, F., Van Hecke, S., Dickinson, D., & Prins, W. (2013) Production and characterization of slow pyrolysis biochar: influence of feedstock type and pyrolysis conditions, *GCB Bioenergy, 5,* 104-115. https://doi.org/10.1111/gcbb.12018.
Sackey, E.A., Song, Y., Yu, Y., & Zhuang, H. (2021) Biochars derived from bamboo and rice straw for sorption of basic red dyes. *PLoS ONE 16(7):* e0254637. https://doi.org/10.1371/journal.
Shaheen, S.M., Niazi, N.K., Hassan, N.E.E., Bibi, I., Wang, H., Daniel, Tsang, C.W., Ok, Y.S., Bolan, N., & Rinklebe, J. (2019) Wood-based biochar for the removal of potentially toxic elements in water and wastewater: a critical review, *Int. Mater. Rev., 64(4)*, 216-247. http://doi.org/10.1080/09506608.2018.1473096,
Singh, H., & Choden, S. (2014) Comparison of Adsorption Behaviour and Kinetic Modeling of Bio-Waste Materials using Basic Dye as Adsorbate. *Indian J. Chem. Technol., 21,* 359–367.

Song, X., Li, Y., Yue, X., Hussain, Q., Zhang, J., Liu, Q., Jin, S., & Cui, D. (2019) Effect of cotton straw-derived materials on native soil organic carbon. *Sci. Total. Environ., 663,* 38-44. https://doi:10.1016/j.scitotenv.2019.01.311.

Spokas, K.A. (2010) Review of the stability of biochar in soils: predictability of O:C molar ratios, *Carbon Manage. 1(2)*, 289-303. https://doi.org/10.4155/cmt.10.32

Srivatsav, P., Bhargav, B.S., Shanmugasundaram, V., Arun, J., Gopinath, K.P., & Bhatnagar, A. (2020) Biochar as an Eco-Friendly and Economical Adsorbent for the Removal of Colorants (Dyes) from Aqueous Environment: A Review. *Water, 12,* 3561. https://doi:10.3390/w12123561

Wang, X., Guo, Z., Hu, Z., & Zhang, J. (2020) Recent advances in biochar application for water and wastewater treatment: a review. *PeerJ 8*:e9164 http://doi.org/10.7717/peerj.9164

Windeatt, J.H., Ross, A.B., Williams, P.T., Forster, P.M., Nahil, M.A., & Singh, S. (2014) Characteristics of biochars from crop residues: Potential for carbon sequestration and soil amendment. *J. Environ. Manag., 146,* 189–197.

Yazdani, M.R., Duimovich, N., Tiraferri, A., Laurell, P., Borghei, M., Zimmerman, J.B., & Vahala, R. (2019) Tailored mesoporous biochar sorbents from pinecone biomass for the adsorption of natural organic matter from lake water. *J. Mol. Liq., 291,* 111248. https://doi.org/10.1016/j.molliq.2019.111248

Yehia, H.M.A.-S., & Said, S.M. (2021) Drinking Water Treatment: pH Adjustment Using Natural Physical Field. *J. Biosci. Med., 9,* 55-66. https://doi.org/10.4236/jbm.2021.96005.

Zhang, X., Gao, B., Zheng, Y., Hu, X., Creamer, A.E., Annable, M.D., & Li, Y. (2017) Biochar for volatile organic compound (VOC) removal: Sorption performance and governing mechanisms. *Bioresour. Technol., 245*, 606-614. http://dx.doi.org/10.1016/j.biortech.2017.09.025

Zhang, J., Lu, F., Zhang, H., Shao, L., Chen, D., & He, P. (2015) Multiscale visualization of the structural and characteristic changes of sewage sludge biochar oriented towards potential agronomic and environmental implication. *Sci Rep 5,* 9406. https://doi.org/10.1038/srep0940616